Tracking Hurricane Claudette with the U.S. Air Force Over-the-Horizon Radar

T. M. GEORGES

NOAA Wave Propagation Laboratory, Boulder, Colorado

J. A. HARLAN

CIRES, University of Colorado, Boulder, Colorado

L. R. MEYER

General Electric Company, Bangor, Maine

R. G. PEER

U.S. Air Force, Northeast Air Defense Sector, Bangor Air National Guard Base, Maine

(Manuscript received 27 August 1992, in final form 9 February 1993)

ABSTRACT

Hurricane Claudette was successfully tracked for three days using the 2-s (7 m) surface wave direction field mapped by the U.S. Air Force OTH-B over-the-horizon radar 2400 km away on the coast of Maine. Inflow and fine structure of the surface circulation are apparent in streamline plots derived from surface wave direction measured with 60-km resolution in the vicinity of the storm for five radar runs. The radar-derived track is within 60 km of that published by the NOAA National Hurricane Center.

1. Introduction

Meteorological and oceanographic remote sensing offers convenient and economical alternatives to conventional weather observations, particularly over large, data-sparse ocean areas. To illustrate the potential of one such remote sensor, we devised a test to see if the new U.S. Air Force OTH-B over-the-horizon early-warning radar system could be used to map the surface circulation of an Atlantic hurricane, and to independently track its center. Although hurricanes have been tracked with such radars before (the physics is not new), this test shows that ocean monitoring can be carried out by piggybacking on this existing operational Air Force radar, without interfering with its military surveillance tasks. The attractive and unique property of the combined East and West Coast OTH-B system is its nominal ocean coverage area of about 40 million square kilometers.

a. Background—Ocean monitoring with OTH radar

Over-the-horizon (OTH or skywave) radars sense natural and man-made targets beyond the optical horizon to ranges of thousands of kilometers by bouncing dekametric radio waves off the ionosphere. Although the technology has been developed primarily for long-range military surveillance (Boutacoff 1985; Headrick 1990), the vast areas accessible to such radars lend them to efficient environmental monitoring as well (Croft 1972). In particular, echoes from the sea that are normally discarded as "clutter" in military applications of OTH radar can be processed to display properties of the sea surface and synoptic weather over large ocean areas (Ahearn et al. 1974; Parent and Gaffard 1976; Dexter and Casey 1978; Georges 1980; Maresca and Georges 1980; Anderson 1986).

b. Tropical storm tracking

After Long and Trizna (1973) and Stewart and Barnum (1975) showed how to map surface wind direction using skywave radar echoes from the sea, Maresca and Barnum (1979) and Maresca and Carlson (1977, 1980) used the same principle to map the surface circulation patterns of tropical storms in the Gulf of Mexico, using the SRI-WARF (Wide Aperture Research Facility) radar in California. Their radar-derived storm tracks compared favorably with those published by the NOAA National Hurricane Center (NHC).

More recently, Anderson (1986, 1990) and Keenan and Anderson (1987) demonstrated that the Australian

Corresponding author address: Dr. T. M. Georges, R/E/WP1, National Oceanic and Atmospheric Administration, 325 Broadway, Boulder, CO 80303-3328.

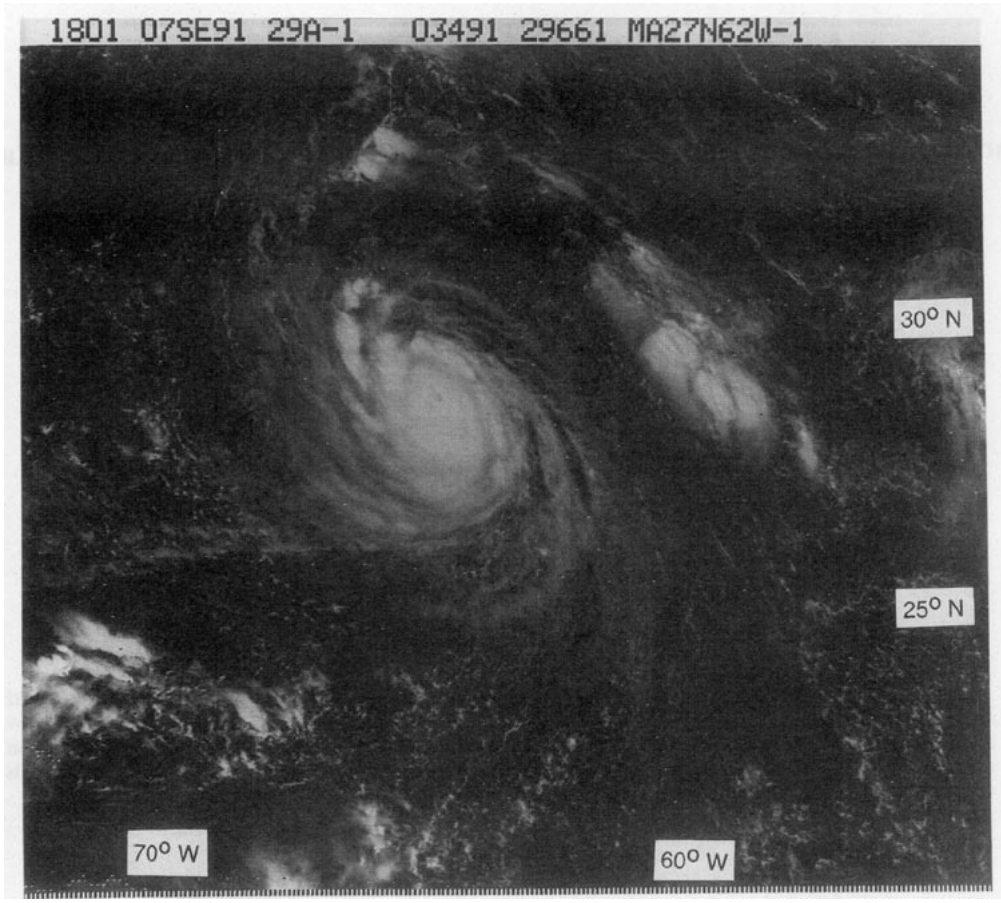

FIG. 1. *GOES-7* image of Hurricane Claudette at the time of radar run 3 (Table 2).

OTH radar known as Jindalee can produce wind-direction maps with 40-km resolution. These maps are transmitted routinely to the Australian Bureau of Meteorology, where they are used to monitor cyclogenesis off that country's northwest coast. Instances have been recorded where OTH radar maps of the surface circulation have helped Australian forecasters distinguish developing tropical storms from nonstorm cyclonic patterns appearing in satellite imagery.

c. Storm history

Hurricane Claudette developed over the subtropical Atlantic and, although small, was quite intense for a brief period. It began life as Tropical Depression Six and was declared a hurricane when its maximum sustained winds exceeded 33.5 m s^{-1} (75 mph) at 1200 UTC 6 September 1991. At that time the storm center was at 26.2°N, 58.8°W (about 1111 km southeast of Bermuda) and was headed west at 3.5 m s^{-1} (8 mph). The NOAA NHC track of Claudette is shown later in Fig. 8, and a *GOES-7* image is shown in Fig. 1. Claudette's winds reached 50.6 m s^{-1} (115 mph) as it turned north and passed 204 km (110 n mi) east-southeast of Bermuda and slowly dissipated as it moved northeastward into temperate latitudes. The minimum surface pressure associated with this storm was 944 mb at 1000 UTC 7 November when the storm center was at 27.0°N, 61.5°W. Claudette spent its entire lifetime at sea, and no damage was documented.

2. Physics of the measurements

In the first-order theory of high-frequency (hf) backscatter from the sea (Wait 1966; Barrick 1972a, 1972b), radar waves backscatter primarily from the ocean waves of one-half the radar wavelength—in other words, from waves that satisfy the Bragg backscatter condition. For a 20-MHz radar, for example, the ocean waves that contribute most to the backscatter cross section are 7.5 m long, travel at a phase speed of 3.4 m s^{-1}, have a period of 2.2 s, and travel exactly toward and away from the radar. Out of the chaos that is the ocean surface, then, the radar "sees" mainly these waves. The spectral signature of the Bragg resonant ocean waves is two sharp peaks in the echo spectrum, shifted from zero by ±0.45 Hz in our example.

Barrick also showed that the relative strengths of the

Bragg line echoes indicate the relative amplitudes of the advancing and receding 7.5-m ocean waves, a measurement that is independent of unknown radar propagation losses.

a. *Surface wave and wind direction from Bragg line ratio*

All methods for estimating the direction θ of the Bragg resonant surface waves (and by inference, surface wind direction) from a single-radar Bragg line ratio R depend on fitting two radar measurements of R (180° apart) to an assumed model, $G(\theta)$, for the angular spreading of short wind-driven ocean waves. Such a fit determines the angle θ between the direction of travel of the strongest Bragg resonant waves and the radar-look direction. If the Bragg resonant waves (of nominally 2-s period) are closely coupled with the local (within 50 km) winds, then θ gives the surface wind direction as well.

All these assumptions are, of course, questionable, and better models of short wind-wave generation are needed. Not only is $G(\theta)$ not well known by oceanographers, but it depends on wind speed, fetch, and duration, and on wave period as well. Another fault of this method is that 2-s waves may not reliably indicate local wind direction when strong winds from nearby weather systems drive significant 2-s wave energy into the radar cell.

In view of uncertainties about $G(\theta)$ and its dependence on wind properties, for the purposes of this paper we make the very simple and tentative assumption that θ is linearly related to $\log R$, if we measure θ from the radar-look direction. Specifically, $\theta = 0°$ when $R = -24$ dB, $\theta = 90°$ when $R = 0$, and $\theta = 180°$ when $R = 24$ dB. This linear law lies in between the laws derived by Long and Trizna (1973), Ahearn et al. (1974), and Stewart and Barnum (1975). It should be possible to derive an improved empirical law by comparison of radar measurements of R with numerical weather prediction models and with large numbers of in situ wind measurements by ships and buoys, and this effort is under way.

TABLE 1. Radar parameters for hurricane tracking.

Modulation	FM-CW
Waveform repetition frequency	10 Hz
Waveform bandwidth	10 kHz
Coherent integration time	12.8 s
Transmitter power	−6 dB re 1 MW
Nominal transmit beamwidth	7.5°
Nominal receive beamwidth	1.25°
Radar frequency	17–21 MHz
Elemental radar cell	1.25° × 15 km
Number of range cells	64
Number of Doppler bins	128 (−5 to +5 Hz)
Number of simultaneous dwells	2
Slant range extent	959 km
Number of receive beams per dwell	3 (1.25° each)
Number of revisits	typically 10–15
Processing parameters	
Number of Doppler bins used	32 (−1.25 to +1.25 Hz)
Range cells incoherently averaged	4

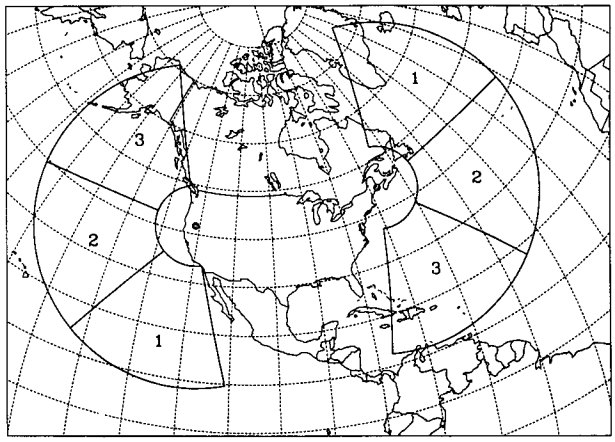

FIG. 2. The nominal one-hop coverage areas of the East and West Coast OTH-B air defense radars operated by the U.S. Air Force, which became operational in 1990. The numbered sectors indicate the contiguous 60° coverage areas of the six independent radars that compose the East and West Coast radar systems. Nominal minimum and maximum one-hop ranges are 926 km (500 n mi) and 3704 km (2000 n mi), giving a 20 million square-kilometer coverage area for each 180° segment. At this writing, the West Coast system has been shut down, and the East Coast system is on limited operational status.

b. *Directional ambiguity*

Determining θ gives only the wind angle from the radar-look direction but not the *sign* of its transverse component. In other words, there is a *left–right ambiguity,* which means that you cannot tell from the Bragg line ratio alone whether the wind is blowing 47° to the right of the radar-look direction or 47° to the left. In the case of hurricanes, this ambiguity can be readily resolved using continuity and global properties of the data field alone (section 4a). For more complicated synoptic fields, independent meteorological or oceanographic data (approximate locations of highs, lows, fronts, etc.) are useful. Measurements from more than one radar can also resolve the ambiguity.

3. Experimental procedure

This one-time demonstration was a cooperative venture between NOAA and the U.S. Air Force Electronics Systems Division. After determining that a hurricane had entered the OTH-B coverage area, we operated one East Coast OTH-B radar in a limited-area ocean-scanning mode during five 1-h periods spaced over 3 days. Ocean scanning was interleaved from minute to minute with aircraft-tracking tasks on a noninterfering schedule. Waveform parameters (Table 1) were selected from those operationally available, and Doppler spectra were recorded on magnetic tape

for postprocessing. No on-line hurricane-tracking capability yet exists on the OTH-B system.

a. The OTH-B radar

The U.S. Air Force AN/FPS-118 or OTH-B air defense radar is by several criteria the largest radar in the world. It is actually six independent over-the-horizon Doppler radars. Three are collocated in the state of Maine on the United States east coast (the East Coast Radar System or ECRS), and the other three (called the WCRS) are collocated near the California–Oregon border. Each radar covers a 60° sector extending between the 926- and 3704-km (500–2000 n mi) ranges, so that the combined 180° coverage area of each three-radar system is about *20 million square kilometers.* Figure 2 shows the nominal coverage areas of the ECRS and WCRS for one ionospheric bounce.

Each transmitting antenna array is 1.1 km long (Fig. 3), and each receiving array is 1.5 km long (Fig. 4). Each radar transmitter is capable of 1-MW frequency modulated-continuous wave (FM-CW) power output into a 7.5° beam that is steerable in azimuth and broad in elevation. The steerable receive beam is nominally 2.5° wide in azimuth but can be narrowed to 1.25° at the expense of higher side-lobe levels. This narrow-beam mode was used for the hurricane test.

The measurements described here were made using the ECRS segment 3 radar concurrently with aircraft-tracking tasks. Its receive antenna array is located at 44.79°N, 67.79°W and covers a 60° sector between 136.5° and 196.5° east of north. Table 1 gives some of the radar operating parameters used for the hurricane experiment.

b. Tracking method

We decided to track Claudette on 5 September 1991 when it entered the radar's coverage area with 16 m s^{-1} winds and the National Hurricane Center forecast an intensifying storm. Tracking began at 1700 UTC 6 September just as Claudette was declared a hurricane by the NHC. During the next three days, five radar snapshots of about 1-h "exposure" were taken of Claudette's surface circulation. The location of the eye of Claudette was determined by telephoning the tropical storm information recording provided by the NHC. These recordings generally update locations every 6 h from satellite imagery and aircraft penetrations. With this independent information about Claudette, radar

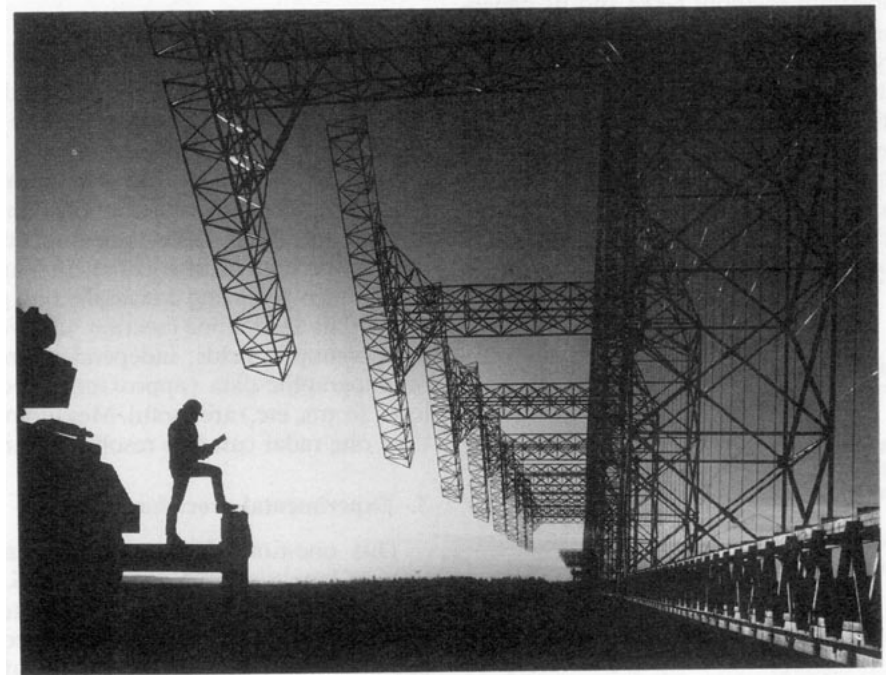

FIG. 3. A portion of one of three transmitting antennas at the OTH-B East Coast Radar System (ECRS) near Moscow, Maine. Each array is 1.1 km long and consists of six 12-element subarrays for transmitting in different frequency bands from 6 to 28 MHz. (The actual frequency used at any given time is determined by ionospheric conditions.) A steerable transmit beam is approximately 7.5° wide in azimuth and broad in elevation. The canted-dipole transmitting elements project in front of a common backscreen between 11 and 41 m high, and a common groundscreen extends 230 m in front of the array. (Photo provided by the General Electric Company.)

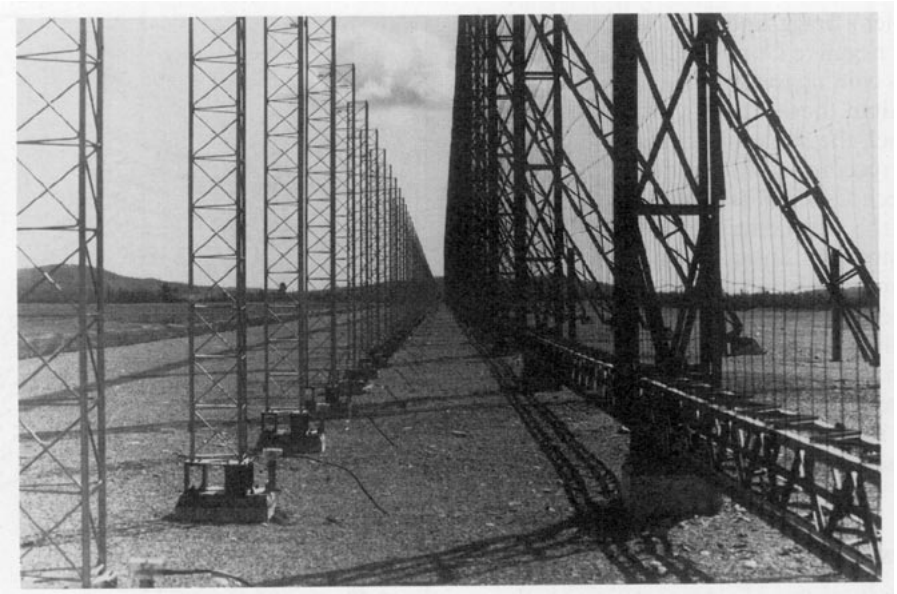

FIG. 4. A portion of one of three receiving antenna arrays of the OTH-B East Coast Radar System near Columbia Falls, Maine. The array is 1.5 km long and consists of 246 monopole elements (to the left) and a 20-m backscreen (right). The nominal azimuthal beamwidth is 2.5°, but a 1.25° beam can be formed by changing the array tapering to a uniform one and accepting higher sidelobe levels. The beam can be electronically steered over a 60° azimuth sector. (Photo provided by the General Electric Company.)

dwell regions were set up, two at a time, to cover the ocean region within roughly 400 km of the storm center. A dwell region, containing three receive beams, covers a 3.75° × 959-km sector, and a 12.8-s coherent integration time was used to resolve the Bragg lines.

Although we used the NHC track to guide the positioning of the radar dwell regions, this was mainly for convenience and saved radar time. There is nothing to prevent scanning larger ocean areas to locate a tropical storm if its position were poorly known.

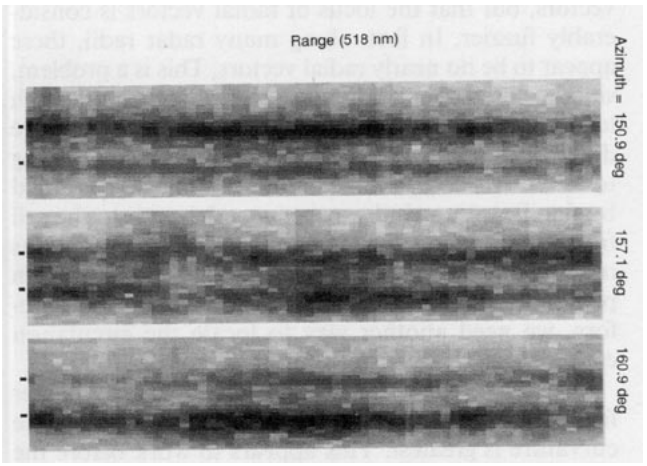

FIG. 5. A range–Doppler plot for radar run 1, showing how the Bragg lines in the sea echo are shifted and spread in frequency by reflection from an irregular ionosphere. Tick marks at the left indicate the theoretical Doppler shifts of the sea-echo Bragg lines, and the Doppler-shift scale goes from +1.25 to −1.25 Hz. The relative strengths of the advancing and receding Bragg lines in the three beams reveal the circulation of Claudette. Radar frequency is 17 MHz.

c. *Ionospheric distortion*

Raw radar spectra show how the sea-echo spectrum is distorted by ionospheric motions and focusing, and illustrate the need for sophisticated signal processing. Figure 5 displays sea-echo spectra in a gray-scale range–Doppler display, in which darkness is proportional to the log of echo intensity. Three panels correspond to three (nonadjacent) 1.25° azimuth beams.

In the absence of ionospheric effects, this display would show two sharp black lines (with some superimposed noise due to the randomness of the sea surface), exactly at the Bragg frequencies (indicated by the tick marks at the left), covering the whole range extent. The actual data show the distortion (spreading and shifting) of the sea echo by the motions of the ionospheric reflecting layer. This space–time variability of the sea echo, combined with superimposed and shifted images due to ionospheric multipath, is what makes processing OTH radar spectra a challenge. This is a typical example; some data are much "cleaner," while other data are hopelessly distorted. This plot shows why it is necessary to sort the data using a quality index and to incoherently average spectra over several radar cells.

These three range–Doppler plots for three azimuth beams clearly show the effects of Claudette's circulation on the radar echo spectrum. In the top panel, the upper

(positive Doppler) Bragg line is consistently stronger than the lower (negative Doppler) line, indicating that the ocean waves coming toward the radar are scattering more strongly than those receding from the radar. In the bottom panel, the situation is reversed, indicating stronger waves receding from the radar. In the center panel, the two echoes are nearly equal, on the average, indicating that the advancing and receding waves are of about equal strength. This is true if the wind is blowing in a direction transverse to a radius from the radar. The picture, then, is of a cyclonic circulation whose center is roughly at the azimuth of the center radar beam. Although it is tempting to interpret the (darker) areas of enhanced echo strength at some ranges as indicating higher seas driven by Claudette, ionospheric focusing can also cause the echo strength to vary with range.

d. Signal processing

Doppler spectra are first incoherently averaged over four range cells to smooth the randomness caused by the ocean surface and by ionospheric motions. This gives a nominally square resolution cell of about 60 km × 60 km. Next, an objective quality index is used to edit the data, discarding spectra falling below a preset quality threshold. The index quantifies how closely each averaged spectrum matches the theoretical Bragg line signature, that is, two sharp lines spaced by $0.2\sqrt{f}$, where f is the radar frequency in MHz. The Bragg line ratio is estimated for the surviving spectra and its values are assigned to the latitude and longitude of the appropriate radar cells. Usually, more than one R value is obtained for a radar cell, because cells are interrogated many times during a scan. The final R assigned to a cell is therefore a quality-weighted average.

4. Analysis of the *R* fields

Figure 6 illustrates the surface wind directions for one Claudette radar run, using the linear transformation (section 2a) between R and wind angle from the radar-look direction. No closed circulation is evident at this point, because the transverse (viewed from the radar) component has been assumed westward for the whole field. Our task now is to resolve the left–right ambiguity, that is, to determine the correct sign of the transverse component of each vector.

Although the sign of the transverse component of a single wind direction measurement cannot be determined without independent information, global properties of the direction field can often be used to construct an unambiguous flow field without recourse to external information.

For example, if we assume only that the center of a closed circulation lies within a data field (e.g., of Fig. 6), then we expect to find a locus of nearly transverse vectors and a locus of nearly radial vectors (again, viewed from the radar). The circulation center would

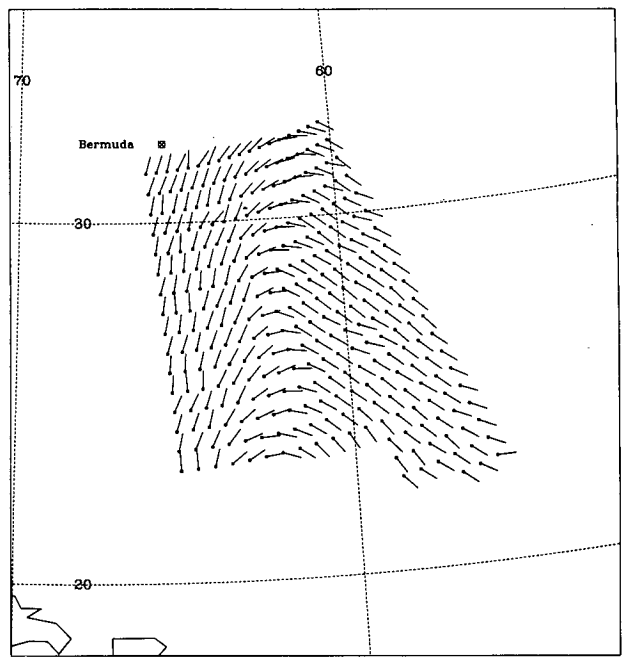

FIG. 6. Map of 2-s surface wave direction for radar run 3, before the left–right radar ambiguity is removed.

lie at the intersection of these two loci. When crossing the locus of radial vectors, the transverse component changes sign, so that inside the locus we would select one sign, and outside we would select the other sign. In this case, it is clear from the radial components (which are not ambiguous) that the signs should be selected to produce a counterclockwise circulation.

If we try this with the direction map of Fig. 6, we find that we can easily identify the locus of transverse vectors, but that the locus of radial vectors is considerably fuzzier. In fact, along many radar radii, there appear to be no nearly radial vectors. This is a problem, since a closed circulation must possess at least one such locus. Some of the indicated directions must therefore differ from purely radial for reasons that have nothing to do with the local wind conditions. This can be caused by significant upwind wave energy driven into the cell from strong winds in neighboring cells, or by variations in wind and wave direction within a 60-km cell. Both possibilities are reasonable within hurricanes. Therefore, we need another way to locate the circulation center along the locus of transverse vectors.

A better method for finding the circulation center from the R field alone is to find where the streamline curvature is greatest. This appears to work before the left–right ambiguity is resolved, and even if the streamlines are significantly noncircular. As an approximation to streamline curvature, we compute the derivative of R with respect to radar azimuth. Contours of this derivative for one radar run are shown in Fig. 7; contours for the other runs are shown in the technical report by

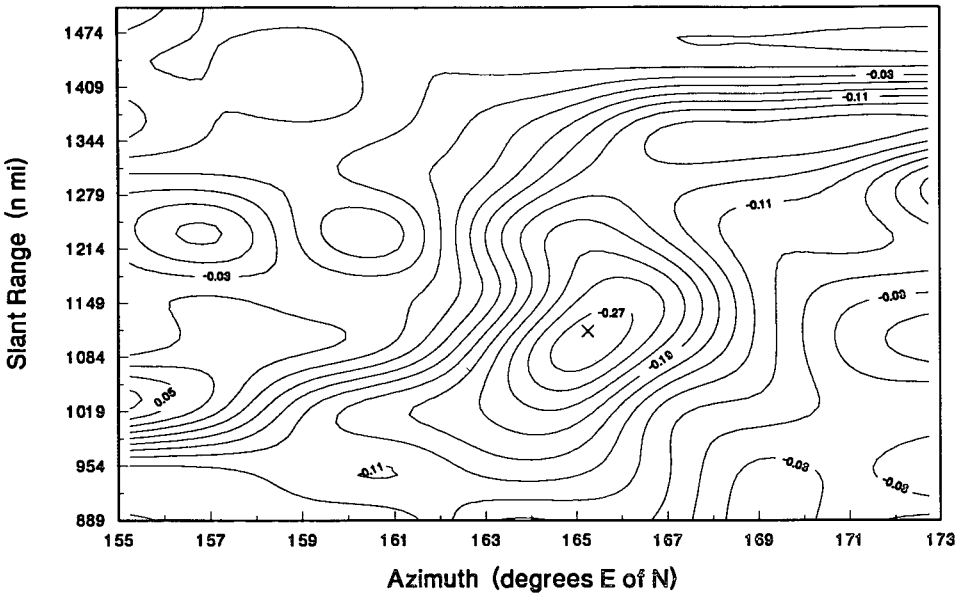

FIG. 7. Contours of the azimuthal derivative of the Bragg line ratio R for radar run 3 (1731–1821 UTC 8 September 1991). The contours are approximately contours of streamline curvature. The "×" marks the radar coordinates of the location of maximum curvature.

Georges et al. (1992). The location of the largest derivative is indicated by "×." These derivative contours reveal peaks in range and azimuth whose sharpness varies from run to run. The radar-derived circulation center is therefore identified as the intersection of the range of maximum curvature with the $R = 0$ locus (transverse wind direction).

5. Results

The main results of this test are (a) a comparison of the OTH-radar track of Claudette with the NHC track, and (b) five surface circulation maps for the five radar runs.

a. Hurricane tracks

Table 2 gives the interpolated NHC locations of the eye of Claudette at the times of the five radar runs. Also given are the radar-derived storm-position estimates for the same times. Figure 8 shows the geographic locations of the NHC (circles) and OTH-B (×'s) centers, along with the NHC track of Claudette in the OTH-B segment 3 coverage area.

b. Surface circulation

Five maps of surface circulation at the times of the five radar runs have been produced. An example is shown in Fig. 9; the remaining four are shown in the technical report by Georges et al. (1992). The circulation centers have been found and the left–right ambiguity has been resolved by the method described in section 4a, that is, by finding the range of maximum streamline curvature and choosing flow from the left (again, viewed from the radar) at shorter ranges and flow from the right at longer ranges. At exactly the range of maximum curvature, the left–right choice is split at the center in favor of the skewness indicated in the contour plots.

The blank areas show where data have been edited out using objective quality criteria. Low data quality is usually the result of poor ionospheric propagation. Although a few obvious outlyers are evident, the overall

TABLE 2. Claudette tracking results.

Run	Date	Julian day	Times (UTC)	NHC position	OTH-B position
1	6 September 1991	249	1723–1800	26.4°N, 59.7°W	26.3°N, 59.8°W
2	7 September 1991	250	1404–1505	27.4°N, 62.0°W	26.9°N, 62.1°W
3	7 September 1991	250	1816–1909	27.8°N, 62.4°W	27.8°N, 62.9°W
4	8 September 1991	251	1230–1339	30.1°N, 63.3°W	30.6°N, 63.3°W
5	8 September 1991	251	1731–1821	31.0°N, 63.2°W	31.2°N, 63.4°W

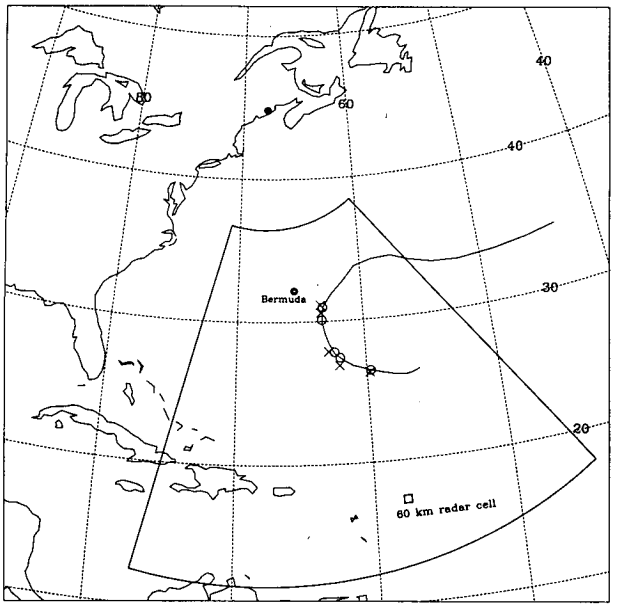

FIG. 8. Map showing the National Hurricane Center track of Hurricane Claudette and the nominal one-hop coverage area of the OTH-B segment 3 radar. Circles show the interpolated NHC locations of Claudette's center during the five radar runs on 6–8 September 1991, and the ×'s show the radar estimates of the storm center at the same times.

directional continuity of the data is one measure of their integrity, especially since they have not been spatially smoothed in any way.

Streamlines constructed from the vector fields are shown in Fig. 10 for all five radar runs. Unrealistic "corners" in the flow are probably caused by one or more of the errors discussed next and will be corrected as the method is refined.

6. Sources of error

Errors in inferring wind direction from the Bragg line ratio R can arise from several causes: (a) Measurements of R itself are subject to the statistical fluctuations of the intensity of echoes from the sea surface, and incoherent averaging of independent samples can reduce this kind of error by known amounts (Barrick and Snider 1977). (b) Errors in the assumed relation between R and wind direction reflect ignorance about the directional spreading function for 2-s wind waves. (c) Errors in the R estimate are also caused by variations in the wind forcing and the wave directional spectrum within a radar cell, and by multimodal directional spectra that do not fit a simple model. (d) In high seas, the height of 2-s ocean waves may saturate and distort the $G(\theta)$ pattern, causing the measured R to be less than for unsaturated conditions.

A small range error, no larger than the size of a radar cell in this case, is caused by an uncertainty in the conversion from radar range to ground range. In this experiment, the conversion data, normally derived from real-time ionospheric soundings, were not recorded and we made the conversion based on typical ionospheric heights, assuming no ionospheric tilts. Larger range errors, even when ionospheric soundings are available, can be caused by ionospheric tilts and the fact that midpoint soundings are generally not available, and these must ultimately be dealt with.

7. The future

Two U.S. Air Force over-the-horizon radars known as OTH-B became operational during 1990. Both are ideally situated for monitoring the large, data-sparse areas of the North Atlantic and northeastern Pacific oceans (Fig. 2) and providing surface data, not available from existing or planned satellite data, that strongly influence the weather and climate of the United States. With the end of the cold war, the role of these radars in the nation's defense is being reassessed, and new peacetime uses for these expensive ($750 million each) national resources are being considered to supplement their defense capabilities and perhaps, finally, to realize OTH radar's full potential for routine ocean monitoring.

The most useful enhancement of OTH-B's ocean monitoring capabilities would be an ability to measure wind speed. This capability has been demonstrated with

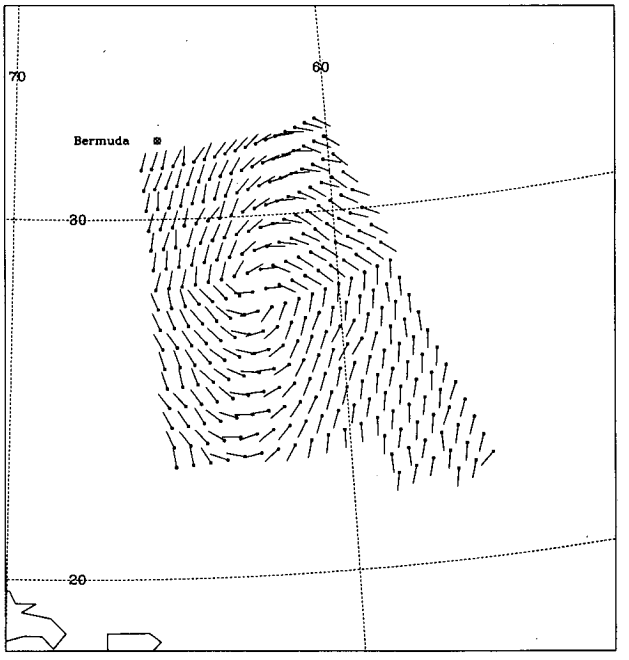

FIG. 9. Surface wind direction vectors for radar run 3 (1816–1909 UTC 7 September 1991), after the left–right ambiguity has been resolved using the streamline-curvature method.

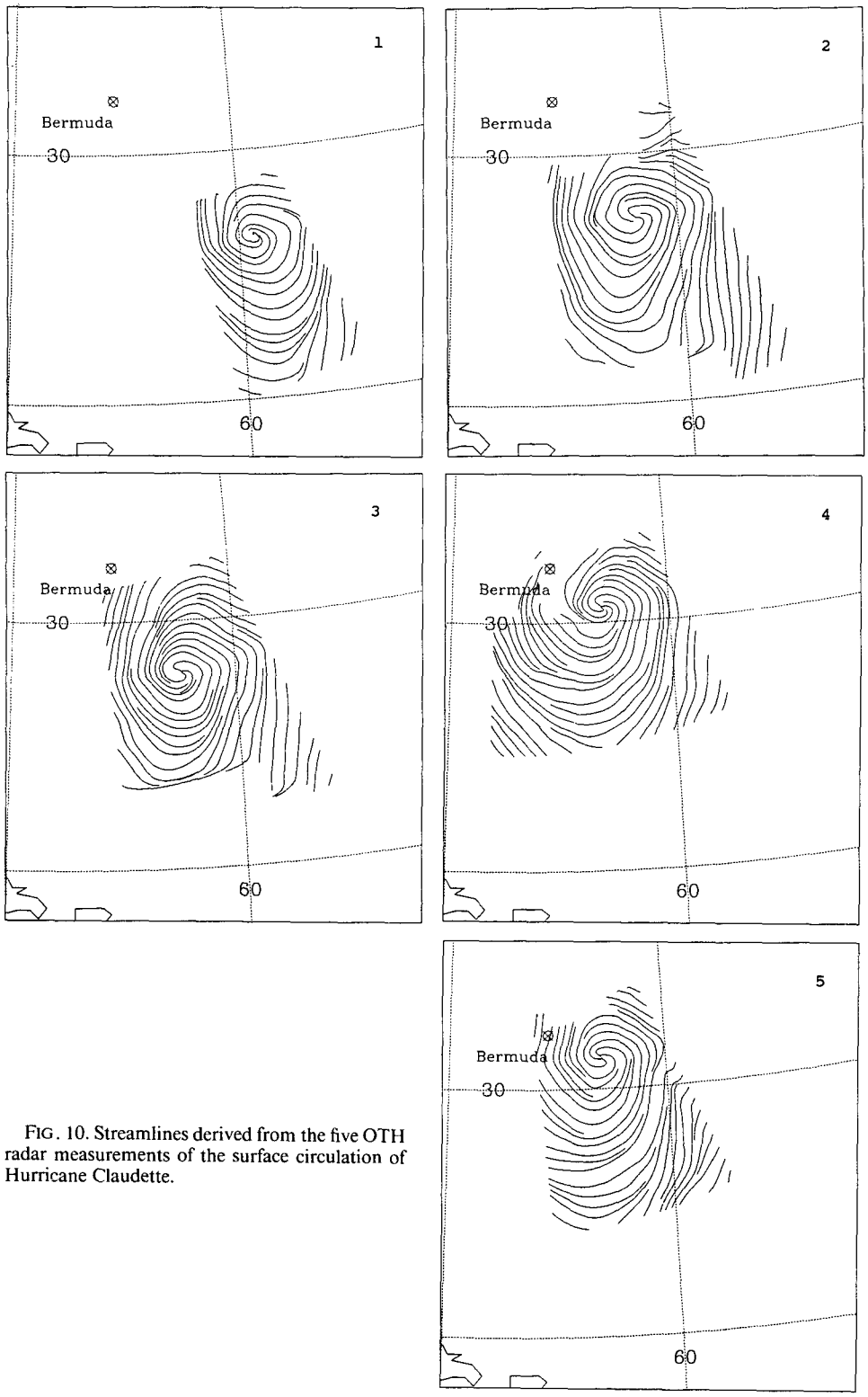

FIG. 10. Streamlines derived from the five OTH radar measurements of the surface circulation of Hurricane Claudette.

research radars (Maresca and Georges 1980; Gaffard and Parent 1990). Only the addition of longer coherent integration times (at least 50 s) to the OTH-B waveforms is required to resolve the second-order spectral features that indicate rms wave height, from which wind speed is inferred.

For such data products to be useful to modelers and forecasters, they must be provided routinely, within hours of the observations. Real-time dissemination of OTH-B ocean surface data will be possible only if (a) the East Coast OTH-B radar continues to operate and (b) an ocean monitoring workstation (OMW) is developed to interface with the radar at the Bangor Operations Center. Using an OMW, an additional operator (either at the Operations Center or at a remote location) could schedule, collect, process, and disseminate large-area ocean surface data in a background mode, without disrupting other radar tasks. Radar-derived surface wind data from its 20 million square-kilometer coverage area would usefully complement satellite and in situ surface wind data, not only for tracking tropical storms, but for monitoring synoptic-scale events as well.

If accurate and routine wide-area hurricane surveillance and tracking by OTH radar is feasible, some measurements now made only through aircraft penetrations of these storms might be accomplished remotely, safely, and more economically. The results presented here and in the Appendix only point the direction toward that goal and, as such, should not be interpreted as indicating the full potential of the technique.

Acknowledgments. This and other ocean monitoring experiments with East Coast and West Coast OTH-B radars were made possible through the courtesy and cooperation of the Air Force Electronics Systems Division (ESD), Hanscom AFB, Massachusetts. In particular, the help and encouragement of Col. Virgil H. Webb, OTH-B Program Director; Lt. Col. Kenneth Marvin; Maj. Leonard Michelson; and Mr. Edward Mahoney of the OTH-B Program Office are deeply appreciated. We are also grateful for the support, hospitality, and interest shown by the military and civilian radar staff at Bangor, particularly Mr. Ray Healy of the General Electric Company and Capt. Jerry Howard, ESD Site Manager. The NOAA National Hurricane Center provided a preliminary report on Claudette as well as the satellite imagery.

Finally, we note with gratitude that the OTH-B facilities and personnel were provided for this and other experiments at no cost to NOAA.

APPENDIX

Observations of Hurricane Andrew

As Hurricane Andrew approached its devastating encounter with southern Florida, we were able to map its surface wind circulation by the same methods already described. A recent rotation of the OTH-B coverage sectors by 15° clockwise permits coverage closer to the Florida coast than had previously been possible. Fig. A1 shows one surface wind direction map of Andrew.

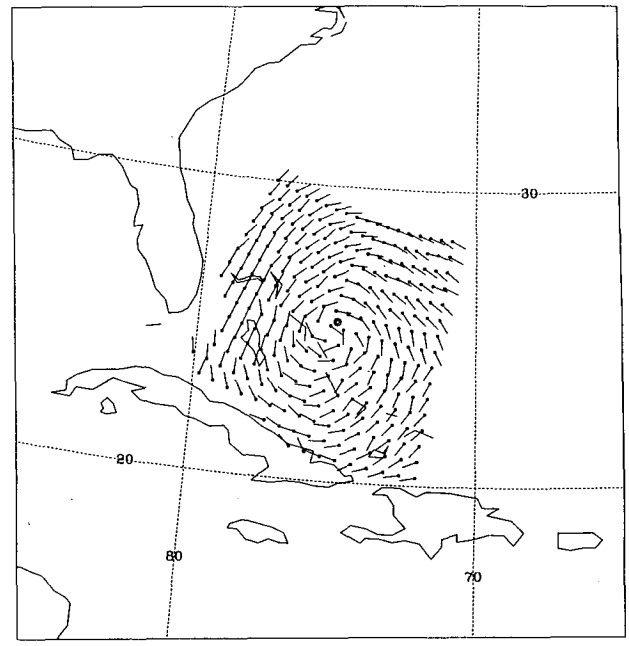

FIG. A1. Wind direction field for Hurricane Andrew derived from OTH-B measurements made between 1521 and 1528 UTC 23 August 1992, using a radar frequency of 15.8 MHz. The circled dot indicates the NHC position estimate at the same time.

REFERENCES

Ahearn, J. L., S. R. Curley, J. M. Headrick, and D. B. Trizna, 1974: Tests of remote skywave measurements of ocean surface conditions. *Proc. IEEE,* **62,** 681–687.

Anderson, S. J., 1986: Remote sensing with the Jindalee skywave radar. *IEEE J. Ocean. Eng.,* **11,** 158–163.

——, 1990: HF skywave radar measurements of cyclone-generated ocean waves. Preprints, RADARCON-90, Adelaide, South Australia.

Barrick, D. E., 1972a: First-order theory and analysis of MF/HF/UHF scatter from the sea. *IEEE Trans. Antennas Propag.,* **40,** 2–10.

——, 1972b: Remote sensing of sea state by radar. *Remote Sensing of the Troposphere,* V. E. Derr, Ed., U.S. Govt. Printing Office, Washington, D.C., 46 pp.

——, and J. B. Snider, 1977: The statistics of HF sea-echo Doppler spectra. *IEEE Trans. Antennas Propag.,* **25,** 19–28.

Boutacoff, D. A., 1985: Backscatter radar extends early warning times. *Defense Electronics,* **17**(5), 71–83.

Croft, T. A., 1972: Sky-wave backscatter: A means of observing our environment at great distance. *Rev. Geophys. Space Phys.,* **10,** 73–155.

Dexter, P. E., and R. Casey, 1978: Ocean windfield mapping at long ranges with an HF radar. *Aust. Meteor. Mag.,* **26,** 33–44.

Gaffard, C., and J. Parent, 1990: Remote sensing of wind speed at sea surface level using HF skywave radar from decametric waves. *Geophys. Res. Lett.*, **17,** 615–618.

Georges, T. M., 1980: Progress toward a practical skywave sea-state radar. *IEEE Trans. Antennas Propag.*, **28,** 751–761.

——, J. A. Harlan, L. R. Meyer, and R. G. Peer, 1992: Tracking hurricane Claudette with the U.S. Air Force OTH-B radar. NOAA Tech. Memo., ERL WPL-219, 39 pp.

Headrick, J. M., 1990: Looking over the horizon. *IEEE Spectrum,* **27,** 36–39.

Keenan, T. D., and S. J. Anderson, 1987: Some examples of surface wind field analysis based on Jindalee skywave radar data. *Austr. Meteor. Mag.*, **35,** 153–161.

Long, A. E., and D. B. Trizna, 1973: Mapping of North Atlantic winds by HF radar backscatter interpretation. *IEEE Trans. Antennas Propag.*, **21,** 680–685.

Maresca, J. W., Jr., and J. R. Barnum, 1979: Remote measurements of the position and surface circulation of hurricane Eloise by skywave radar. *Mon. Wea. Rev.*, **107,** 1648–1652.

——, and C. T. Carlson, 1977: Tracking and monitoring hurricanes by HF skywave radar over the Gulf of Mexico. SRI International Tech. Report, Menlo Park, CA, 118 pp.

——, and ——, 1980: High-frequency radar measurements of hurricane Anita. *Science,* **209,** 1189–1196.

——, and T. M. Georges, 1980: Measuring rms wave height and the scalar ocean wave spectrum with HF skywave radar. *J. Geophys. Res.*, **85**(C5), 2759–2771.

Parent, J., and C. Gaffard, 1976: Detection of meteorological fronts over the North Sea with an HF skywave radar. *IEEE J. Ocean. Eng.*, **11,** 174–179.

Stewart, R. H., and J. R. Barnum, 1975: Radio measurements of oceanic winds at long ranges: An evaluation. *Radio Sci.*, **10,** 853–857.

Wait, J. R., 1966: Theory of HF ground wave backscatter from sea waves. *J. Geophys. Res.*, **71,** 4839–4842.